[3]Bettermann, D., "Contribution a l'Etude de la Convection Force Turbulente le Long de Plaques Rugueuses," *International Journal of Heat and Mass Transfer,* Vol. 9, March 1966, pp. 153-164.

[4]Dvorak, F. A., "Calculation of Turbulent Boundary Layers on Rough Surfaces in Pressure Gradient," *AIAA Journal*, Vol. 7, Sept. 1969, pp. 1752-1759.

[5]Simpson, R. L., "A Generalized Correlation of Roughness Density Effects on the Turbulent Boundary Layer," *AIAA Journal*, Vol. 11, Feb. 1973, pp. 242-244.

[6]Dirling, R. B., Jr., "A Method for Computing Roughwall Heat-Transfer Rates on Re-Entry Nose Tips," AIAA Paper 73-763, July 1973.

[7]Grabow, R. M. and White, C.O., "Surface Roughness Effects on Nose Tip Ablation Characteristics," *AIAA Journal*, Vol. 13, May 1975, pp. 605-609.

[8]Donne, M., and Meyer, L., "Turbulent Convective Heat Transfer from Rough Surfaces with Two-Dimensional Rectangular Ribs," *International Journal of Heat and Mass Transfer,* Vol. 20, June 1977, pp. 583-620.

[9]Coleman, H. W., Hodge, B. K., and Taylor, R. P., "A Reevaluation of Schlichting's Surface Roughness Experiment," *Journal of Fluid Engineering*, Vol. 106, March 1984, pp. 60-65.

[10]Webb, R. L., Eckert, E. R. G., and Goldstein, R. J., "Heat Transfer and Friction in Tubes with Repeated Rib Roughness," *International Journal of Heat and Mass Transfer,* Vol. 14, April 1971, pp. 601-617.

[11]Han, J. C., Glickman, L. R., and Rohsenow, W. M., "An Investigation of Heat Transfer and Friction for Rib-Roughened Surfaces," *International Journal of Heat and Mass Transfer,* Vol. 21, Aug. 1978, pp. 1143-1156.

[12]Liu, C. K., Kline, S. J., and Johnston, J. P., "An Experimental Study of Turbulent Boundary Layer on Rough Walls," Dept. of Mechanical Engineering, Stanford Univ., Rept. MD-15, 1966.

[13]Pineau, F., Nguyen, V. D., Dickinson, J., and Belanger, J., "Study of a Flow Over a Rough Surface with Passive Boundary-Layer Manipulators and Direct Wall Drag Measurements," AIAA Paper 87-0357, 1987.

[14]Perry, A. E., and Joubet, P. N., "Rough-Wall Boundary Layers in Adverse Pressure Gradients," *Journal of Fluid Mechanics,* Vol. 17, Pt. 2, Oct. 1963, pp. 193-211.

[15]Antonio, R. A. and Luxton, R. E., "The Response of a Turbulent Boundary Layer to a Step Change in Surface Roughness, Pt. 1. Smooth to Rough," *Journal of Fluid Mechanics,* Vol. 48, Pt. 4, Aug. 1971, pp. 721-762.

[16]Antonia, R. A., and Wood, D. H., "Calculation of a Turbulent Boundary Layer Downstream of a Step Change in Surface Roughness," *Aeronautical Quarterly,* Vol. 26, Pt. 3, Aug. 1975, pp. 202-210.

[17]Furuya, Y., Fujita, H., and Nakashima, H., "Turbulent Boundary Layers on Plates Roughened by Wires in Equal Intervals," Data Reported by I. Tani in *Perspectives in Turbulence Studies,* Springer-Verlag, Berlin, West Germany, 1987, pp. 223-249.

[18]Sherif, N., and Gumley, P., "Heat-Transfer and Friction Properties of Surfaces with Discrete Roughnesses," *International Journal of Heat and Mass Transfer,* Vol. 9, Dec. 1966, pp. 1297-1320.

Analysis of Transonic Integral Equations: Part II—Boundary Element Methods

W. Ogana*
University of Nairobi, Nairobi, Kenya

Introduction

THE transonic integro-differential and integral equations have normally been solved by constant elements, except in the case of Nixon[1] who solved the equation involving a decay function by using a linear interpolation function to express the transverse variation of the streamwise velocity in each horizontal strip in terms of values on the strip edges. Research in boundary element methods has revealed that constant elements are the simplest of a class of methods and that better accuracy may be achieved by using higher-order elements.[2] In this paper we formulate the boundary element solutions of the two-dimensional transonic integro-differential and integral equations as developed in Part I.[3] Apart from using constant and quadrilateral elements, we develop hybrid elements based on constant elements in the streamwise direction and variable elements in the transverse direction. This leads to constant-linear and constant-quadratic elements. The boundary conditions term is computed using linear and quadratic elements, in addition to constant elements. Computation is carried out for nonlifting parabolic-arc and NACA0012 airfoils.

Received March 27, 1987; revision received Nov. 21, 1988.

*Associate Professor, Department of Mathematics. Member AIAA.

Boundary Element Methods

The basic equations to be solved are Eqs. (5) and (8) of Part I. The computational domain is discretized into surface elements of suitable shapes. We use rectangular elements, with m elements in each of the n horizontal strips. Hence there are $M=mn$ elements denoted $\Delta_1,\Delta_2,\ldots,\Delta_M$, starting from the bottom left and proceeding from left to right in each horizontal strip. Let Δ_j have width $2\delta_j$, height $2h_j$, aspect ratio $\alpha_j=h_j/\delta_j$, and center with coordinates (X_j,Y_j). Solutions are obtained at the N nodes labeled $Q_1,Q_2,\ldots,Q_N$, starting from the bottom left and proceeding from left to right in each row. Let Q_i have coordinates (x_i,y_i).

Uniform treatment can be given to the numerical solution of the integro-differential and integral equations, as shown in Part I. Application of these equations at Q_i yields the nonlinear system

$$\psi_i=\psi_i^B+\sum_{j=1}^{M} I_j, \qquad i=1,2,\ldots,N \tag{1}$$

where

$$I_j=\int\int_{\Delta_j} K(\xi-x_i,\zeta-y_i)H(\xi,\zeta)\ \mathrm{d}S \tag{2}$$

while ψ_i,ψ_i^B, K, and H are defined in Part I. The various boundary element methods depend on how Eq. (2) is approximated.

Constant Elements

We assume that H is constant within Δ_j and takes the value at the node Q_j, appropriately located in Δ_j such that $x_j=X_j$. If Δ_j touches the x axis, the node is located on the x axis, marked ○ and labeled 1 in Fig. 1. Otherwise, the node is located at the center of Δ_j, marked ○ and labeled 3 in Fig. 1. There is one

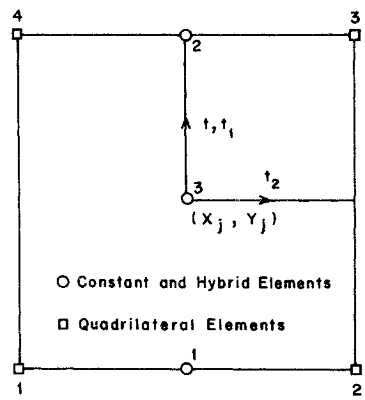

Fig. 1 Location and numbering of nodes within the rectangular element.

node per rectangular element so that $N=M$. Equation (2) reduces to

$$I_j = b_{ij} H_j \tag{3}$$

where $H_j \equiv H(Q_j)$ and

$$b_{ij} = \int_{\Delta_j}\int K(\xi - x_i, \zeta - y_i)\, \mathrm{d}s \tag{4}$$

Hence, Eq. (1) becomes

$$\psi_i = \psi_i^B + \sum_{j=1}^{N} b_{ij} H_j, \qquad i = 1,2,\ldots,N \tag{5}$$

where $[b_{ij}]$ is a matrix of order N. The matrix element b_{ij} may be evaluated by Gaussian quadrature; however, analytical evaluation is straightforward and preferable. This has been the most widely used method to approximate Eq. (2).

Hybrid Elements

Transonic disturbances are known to persist for much longer distances in the transverse than in the streamwise direction. We may, therefore, assume that within each rectangular element H is constant in the streamwise direction and takes the value at the center of the element but is variable in the transverse direction. Define the local coordinates

$$t = (\xi - Y_j)/h_j \tag{6}$$

for Δ_j in the transverse direction. Application to Eq. (2) and evaluation of the integral with respect to ξ yields

$$I_j = \int_{-1}^{1} w^h(a+t, s_1, s_2) H(x_j, t)\, \mathrm{d}t \tag{7}$$

where

$$W^h = \begin{cases} \dfrac{h_j}{8\pi} \ell n \left[\dfrac{s_1^2 + (a+t)^2}{s_2^2 + (a+t)^2} \right] & \text{for the TIDE} \\[2ex] \dfrac{1}{4\pi} \left[\dfrac{s_2}{s_2^2 + (a+t)^2} - \dfrac{s_1}{s_1^2 + (a+t)^2} \right] & \text{for the TIE} \end{cases} \tag{8}$$

in which

$$a = \frac{Y_j - y_i}{h_j}, \quad s_1 = \frac{X_j - x_i - \delta_j}{h_j}, \quad s_2 = \frac{X_j - x_i + \delta}{h_j} \tag{9}$$

The first hybrid method is the constant-linear element for which we assume that $H(x_j,t)$ varies linearly for $t \in [-1,1]$. Hence $H(x_j,t)$ is given by[2]

$$H(x_j, t) = \theta_1^{c\ell} H_{j1} + \theta_2^{c\ell} H_{j2} \tag{10}$$

where H_{j1} and H_{j2} are the values of H at the nodes, in Δ_j, marked o in Fig. 1 and labeled 1 and 2, respectively. The shape functions are given by

$$\theta_1^{c\ell} = \tfrac{1}{2}(1-t) \qquad \theta_2^{c\ell} = \tfrac{1}{2}(1+t) \tag{11}$$

substitution of Eq. (10) into Eq. (7) yields

$$I_j = h_{ij}^1 H_{j1} + h_{ij}^2 H_{j2} \tag{12}$$

where

$$h_{ij}^k = \int_{-1}^{1} \theta_k^{c\ell}(t) W^h(a+t, s_1, s_2)\, \mathrm{d}t \qquad k = 1,2 \tag{13}$$

The quantity h_{ij}^k is an influence coeffeceint which defines the interaction between the node Q_i and a particular node labeled k on Δ_j.

The second hybrid method is the constant-quadratic element. Here we assume that $H(x_j,t)$ varies quadratically for $t \in [-1,1]$. Similar analysis leads to

$$I_j = h_{ij}^1 H_{j1} + h_{ij}^2 H_{j2} + h_{ij}^3 H_{j3} \tag{14}$$

where the influence coefficients are

$$h_{ij}^k = \int_{-1}^{1} \theta_k^{cq}(t) W^h(a+t, s_1, s_2)\, \mathrm{d}t \qquad k = 1,2,3 \tag{15}$$

The shape functions are

$$\theta_1^{cq} = \tfrac{1}{2}t(t-1), \quad \theta_2^{cq} = \tfrac{1}{2}t(t+1), \quad \theta_3^{cq} = (1-t)(1+t) \tag{16}$$

while H_{j1}, H_{j2}, and H_{j3} are the values of H at the nodes, in Δ_j, marked o in Fig. 1 and labeled 1, 2, and 3, respectively.

The influence coefficients in Eqs. (13) and (15) may be evaluated by Gaussian quadrature but analytical integration is straightforward and preferable.

Quadrilateral Elements

For Δ_j, define the local coordinates

$$t_1 = \frac{\xi - X_j}{\delta_j}, \qquad t_2 = \frac{\xi - Y_j}{h_j} \tag{17}$$

and substitute in Eq. (2) to find

$$I_j = \int_{-1}^{1}\int_{-1}^{1} W^q(a_1 + t_1, a_2 + t_2) H(t_1, t_2) \mathrm{d}t_1, \mathrm{d}t_2 \tag{18}$$

where

$$W^q = \begin{cases} -\dfrac{h_j}{4\pi} \dfrac{a_1 + t_1}{(a_1+t_1)^2 + \alpha_j^2 (a_2+t_2)^2} & \text{for the TIDE} \\[2ex] -\dfrac{\alpha_j}{4j} \dfrac{(a_1+t_1)^2 - \alpha_j^2(a_2+t_2)^2}{[(a_1+t_1)^2 + \alpha_j^2(a_2+t_2)^2]^2} & \text{for the TIE} \end{cases} \tag{19}$$

and

$$a_1 = \frac{X_j - x_i}{\delta_j}, \qquad a_2 = \frac{Y_j - y_i}{h_j} \tag{20}$$

For the simplest quadrilateral element we let[2]

$$H(t_1, t_2) = \theta_1^q H_{j1} + \theta_2^q H_{j2} + \theta_3^q H_{j3} + \theta_4^q H_{j4} \tag{21}$$

where H_{j1}, H_{j2}, H_{j3}, and H_{j4} are the values of H at the nodes in Δ_j, marked □ and labeled 1,2,3, and 4, respectively, in Fig. 1. The shape functions are

$$\theta_1^q = \tfrac{1}{4}(1-t_1)(1-t_2) \qquad \theta_2^q = \tfrac{1}{4}(1+t_1)(1-t_2)$$
$$\theta_3^q = \tfrac{1}{4}(1+t_1)(1+t_2), \qquad \theta_4^q = \tfrac{1}{4}(1-t_1)(1+t_2) \tag{22}$$

Substitution of Eq. (21) into Eq. (18) yields

$$I_j = \sum_{k=1}^{4} h_{ij}^k H_{jk} \tag{23}$$

in which the influence coefficient is given by

$$h_{ij}^k = \int_{-1}^{1}\int_{-1}^{1} \theta_k^q(t_1, t_2) W^q(a_1 + t_1, a_2 + t_2)\, \mathrm{d}t_1\, \mathrm{d}t_2 \tag{24}$$

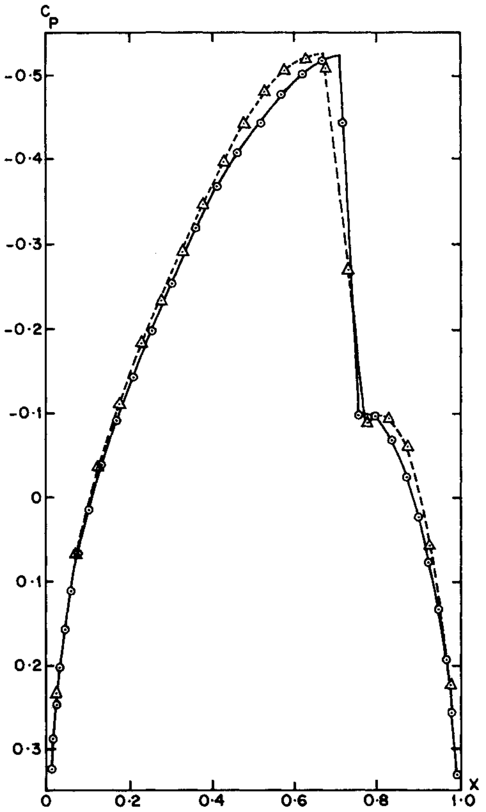

Fig. 2 Coefficient of pressure for a prabolic-arc airfoil of thickness ratio 0.06, at $M_\infty = 0.87$.

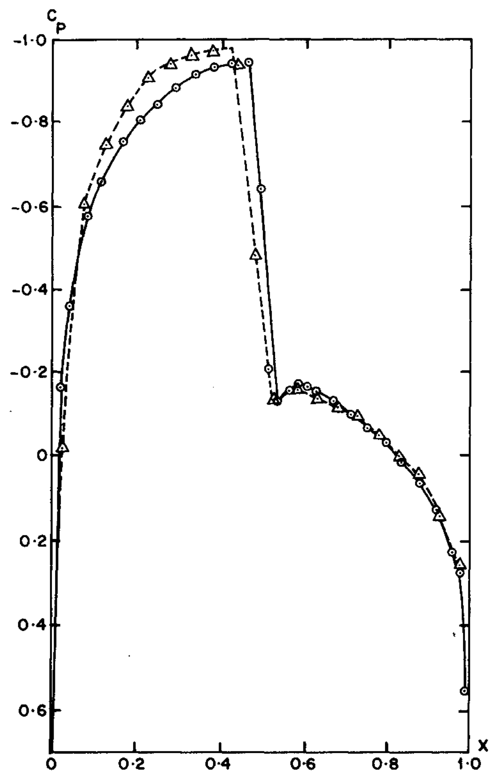

Fig. 3 Coefficient of pressure for NACA0012 at $M_\infty = 0.8$.

If $Q_i \notin \Delta_j$, then Eq. (24) may readily be evaluated by Gaussian quadrature which, for this expression, is more efficient than analytical approach. However, if $Q_i \epsilon \Delta_j$ singularities occur and special quadrature formulas[2] or analytical evaluation can be used. The results for the latter approach are obtained after considerable manipulations.

Results

Before numerical solutions are carried out the system of equations may be put in the form of Eq. (5), where N depends on the type of boundary element. Using the approach presented here, the boundary conditions term ψ^B may be evaluated by linear or quadratic elements, in addition to constant elements. Flows with shocks are solved as described in Part I. Computation was carried out on a Gould 32 computer for nonlifting parabolic-arc and NACA0012 airfoils in subcritical and supercritical flows. The computational domain was discretized with $m = 50$ and n ranging from 1 to 4, depending on the method. Thus, the number of nodes varied from 50–250. Iteration stopped when the relative error between successive iterates of u was less than 0.01 at all nodes. We present only results from constant-linear elements. These values are more accuate than constant elements but slightly less accurate than constant-quadratic elements. Besides, for graphical purposes the difference between the three results is not significant.

Figure 2 shows the coefficient of pressure plots for a parabolic-arc airfoil, obtained from the integral equation; Fig. 3 shows the results for a NACA0012 airfoil, obtained from the integro-differential equation. The finite-difference results for Fig. 2 are due to Ballhaus, Jameson, and Albert,[4] those of Fig. 3 are from Jameson.[5] For the current method, convergence occurred in eight iterations for the TIE and 21 iterations for the TIDE.

Computation was also carried out using one strip of rectangular elements and the results compared with multistrip solutions. Correct to four decimal places, the maximum relative error between multistrip and one-strip results for the parabolic-arc airfoil was 0.0123 for constant elements, 0.0006 for constant-linear elements, and 0.0000 for constant-quadratic elements. For the NACA0012 airfoil, the maximum relative error was 0.0486 for constant elements, 0.0047 for constant-linear elements, and 0.0000 for constant-quadratic elements. We see that hybrid elements, particularly constant-quadratic, yield fairly good results even if one strip of rectangular elements is used. The decay function[6] was also tested, with one horizontal strip of elements, and the results did not show significant departure from the direct multistrip solutions.

References

[1]Nixon, D., "Calculation of Transonic Flows Using an Extended Integral Equation Method," *AIAA Journal*, Vol. 15, March 1977, pp. 295–296.

[2]Brebbia, C. A., Telles, J. C. F., and Wrobel, L. C., *Boundary Element Techniques*, Springer-Verlag, Berlin, Heidelberg, New York, 1984.

[3]Ogana, W., "Analysis of Transonic Integral Equations: Part I—Artificial Viscosity," *AIAA Journal*.

[4]Ballhaus, W. F., Jameson, A., and Albert, J., "Implicit Approximate Factorization Schemes for the Efficient Solution of Steady Transonic Flow Problems," NASA TMX-73202, Jan. 1977.

[5]Jameson, A., "Transonic Airfoil Calculations Using the Euler Equations," *Numerical Methods in Aeronautical Fluid Dynamics*, Academic, London, UK, 1982.

[6]Ogana, W., "Choosing the Decay Function in the Transonic Integral Equations," International Centre for Theoretical Physics, Internal Report, Triest, IT, IC/83/21, Feb. 1983.